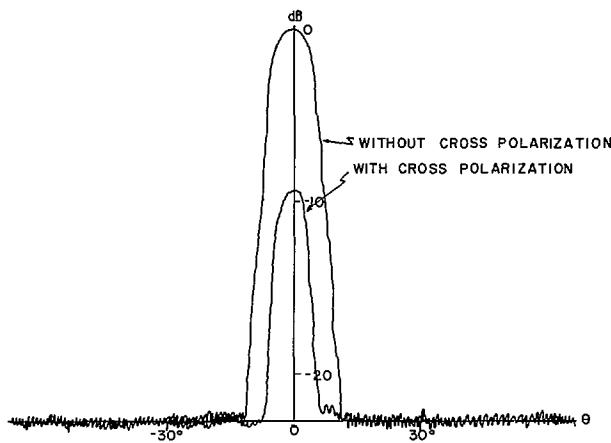Fig. 3.

Fig. 4.

METHOD OF DETECTION

The method of exciting the array discussed previously raises the problem of separating the incident wave from the scattered wave because only the scattered wave (reradiation from array elements) is of interest. In our experiment we used a plane wave to excite the array whose polarization is such that the electric field is spatially oriented at 45 degrees with respect to the dipoles on the array. The reradiated electric field is detected by the receiving antenna which is rotated such that its polarization is at 90 degrees spatially with respect to that of the transmitted wave. This will allow the scattered wave to be received while the incident wave is rejected. This method gives approximately 10 dB decoupling between the incident signal power and the received one (Fig. 4).

The method is further improved by using a microwave bridge circuit. A signal is derived from the plane-wave source in the absence of the array to cancel any signal received by the receiving antenna. Then the array is placed in position to measure the scattered field. With this arrangement the signal re-

ceived directly from the transmitter can be brought down to better than −13 dB in the region around the main beam of the transmitter and beyond −20 dB in other regions.

A block diagram of this experimental setup is shown in Fig. 2, and a typical experimental radiation pattern compared with the theoretical pattern at designed frequency is shown in Fig. 3.

CONCLUSION

We have investigated the radiation pattern of a spherical array by means of the scattered plane resulting from a wave propagating along the polar axis of the sphere. The technique of detecting the scattered field from the sum of the scattered field and incident field is discussed, and some experimental results are shown.

ANDREW K. CHAN
RUBENS A. SIGELMANN
Dept. of Elec. Engrg.
University of Washington
Seattle, Wash. 98105

REFERENCES

[1] A. Chan, A. Ishimaru, and R. Sigelmann, "Equally spaced spherical arrays," *Radio Sci.*, vol. 3, pp. 401–404, May 1968.

Resonant Quadrafilar Helix

Abstract—The radiation of the resonant, fractional-turn, quadrafilar helix is shown to be cardioid shaped and circularly polarized regardless of axial length and diameter. Measured and calculated data relate the radiation pattern characteristics and geometrical parameters.

INTRODUCTION

An earlier paper [1] has shown that the resonant (element length $= \lambda/2$), 1/2-turn, antiphase-fed, bifilar helix radiates a sine-shaped, circularly polarized radiation pattern when the diameter $= 0.18\lambda$ and the axial length $= 0.27\lambda$; and that two such bifilar helices, concentric with orthogonal radials (a quadrafilar helix), radiate a cardioid-shaped, circularly polarized pattern when fed in phase quadrature.

New experimental data indicates that resonant 1/4-turn, 1/2-turn, and 1-turn quadrafilar helices radiate a cardioid-shaped, circularly polarized pattern for all axial lengths and diameters. Pattern shape and axial ratio are degraded for very large or very small axial length/diameter and for helices with more than 1 turn. Graphs of the measured beamwidth, axial ratio, and front-to-back ratio are included, as shown in Fig. 3.

Integral formulas for the radiation of the multielement helix have been derived. The radiation patterns of several helices have been computed by numerical integration and found to agree with the measured data.

ANALYSIS

The variables and parameters used are defined in Fig. 1. The fields of the radials and the fields of the helical portions will be evaluated independently and then summed. The assumed current distribution is sinusoidal with maxima at the feed and the distal end. Utilizing the usual approximations [2], the ϕ component of the total field of element 1 is

$$E_{\phi 1} = \frac{-j\omega\mu e^{-jkr}}{4\pi r} \int_{l=0}^{l=\lambda/2} \bar{i}_\phi e^{jkr' \cos \psi} \, dl.$$

Field of the Helical Portions

Let α be the integration variable. From Fig. 1

$$dl = \frac{r_0 d_\alpha}{\cos \beta}$$

and the general formula is

$$E_{\phi H} = \frac{-j\omega\mu r_0 e^{-jkr}}{4\pi r \cos \beta}$$

$$\cdot \int_{\alpha=0}^{2N\pi} i_\phi(\phi,\alpha) e^{jkr' \cos \psi} \, d\alpha.$$

For each element of the helix the current magnitudes are

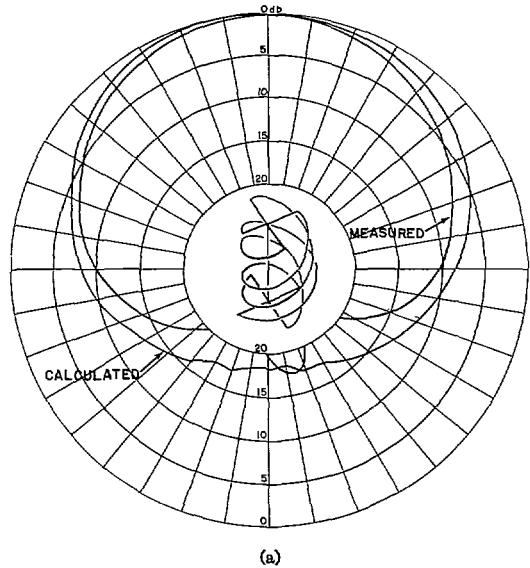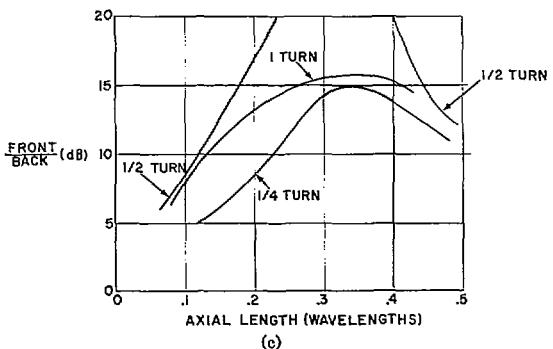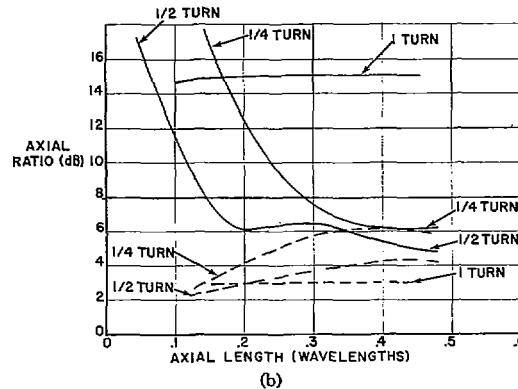$$i_\phi(\alpha) = I_0 \cos (kr_0) \cos \frac{\alpha}{2N} \cos \beta.$$

Fig. 1.

(a)

(b)
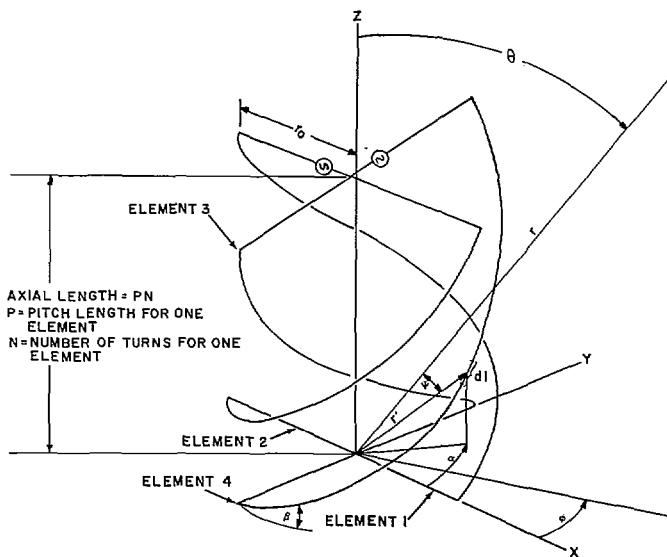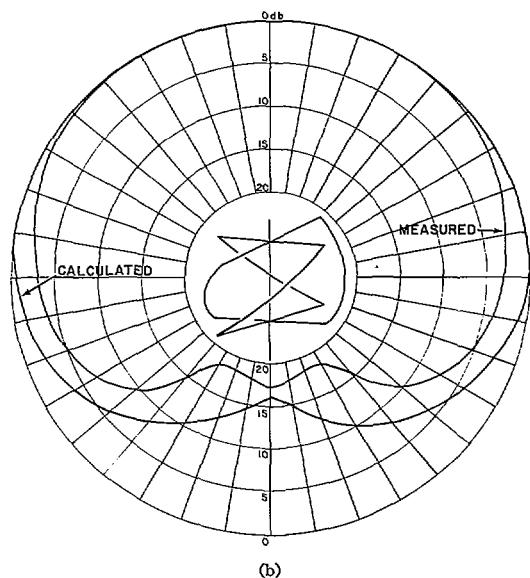
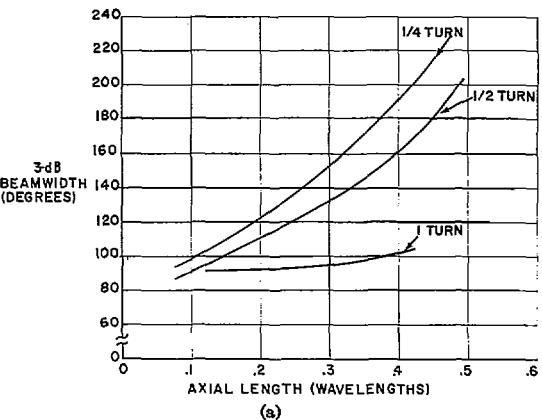Fig. 2.   (a) Quadrafilar helix 1 turn. $\phi = 0$, $P = 0.14\lambda$, $r_0 = 0.06\lambda$. (b) Quadrafilar helix 1/4 turn. $\phi = 0$, $P = 1.36\lambda$, $r_0 = 0.09\lambda$.

(a)

(b)

(c)

Fig. 3.   Quadrafilar helix, experimental data. Solid lines in (c) indicate peak axial ratio over the hemisphere in front of helix; dashed lines indicate peak axial ratio over 3-dB beamwidth of helix.

For elements 1 and 2:

$$i_\phi(\phi,\alpha) = i_\phi(\alpha) \cos(\phi - \alpha).$$

For elements 3 and 4:

$$i_\phi(\phi,\alpha) = i_\phi(\alpha) \sin(\phi - \alpha).$$

The phase term for element 1 is

$$r' \cos \psi = \frac{\bar{r}' \cdot \bar{r}}{r}$$

$$= r_0 \cos \alpha \sin \theta \cos \phi + r_0$$

$$\cdot \sin \alpha \sin \theta \sin \phi + \frac{P\alpha}{2\pi}$$

$$\cdot \cos \theta.$$

Define

$$K = \frac{\omega \mu I_0 r_0 \cos(kr_0) e^{-jkr}}{4\pi r}.$$

Then E_ϕ for the helical portion of element 1 is given by

$$E_{\phi H_1} = -jK \int_{\alpha=0}^{2N\pi} \cos\left(\frac{\alpha}{2N}\right)$$

$$\cdot \cos(\phi - \alpha) \exp\left[jk\left(r_0 \cos \alpha\right.\right.$$

$$\cdot \sin \theta \cos \phi + r_0 \sin \alpha \sin \theta \sin \phi$$

$$\left.\left. + \frac{P\alpha}{2\pi} \cos \theta\right)\right] d\alpha.$$

Similarly, the field of element 2 is

$$E_{\phi H_2} = -jK \int_{\alpha=0}^{2N\pi} \cos\left(\frac{\alpha}{2N}\right)$$

$$\cdot \cos(\phi - \alpha) \exp\left[jk\left(-r_0 \cos \alpha\right.\right.$$

$$\cdot \sin \theta \cos \phi - r_0 \sin \alpha \sin \theta \sin \phi$$

$$\left.\left. + \frac{P\alpha}{2\pi} \cos \theta\right)\right] d\alpha.$$

Elements 3 and 4 (the second bifilar helix) are fed in phase quadrature, to elements 1 and 2, respectively. The fields are

$$E_{\phi H_3} = K \int_{\alpha=0}^{2N\pi} \cos\left(\frac{\alpha}{2N}\right) \sin(\phi - \alpha)$$

$$\cdot \exp\left[jk\left(-r_0 \sin \alpha \sin \theta \cos \phi\right.\right.$$

$$+ r_0 \cos \alpha \sin \theta \sin \phi$$

$$\left.\left. + \frac{P\alpha}{2\pi} \cos \theta\right)\right] d\alpha$$

$$E_{\phi H_4} = K \int_{\alpha=0}^{2N\pi} \cos\left(\frac{\alpha}{2N}\right) \sin(\phi - \alpha)$$

$$\cdot \exp\left[jk\left(r_0 \sin \alpha \sin \theta \cos \phi\right.\right.$$

$$- r_0 \cos \alpha \sin \theta \sin \phi$$

$$\left.\left. + \frac{P\alpha}{2\pi} \cos \theta\right)\right] d\alpha.$$

Field of the Radials

If the current on the radials is approximated by a uniform distribution, the following simplified solutions result:

1/4-turn helix

$$E_{\phi R1,2} = \frac{-j\omega \mu e^{-jkr}}{4\pi r} 2r_0 I_0$$

$$\cdot (\cos \phi\, e^{jk \cos \theta\, P/4} - \sin \phi)$$

$$E_{\phi R3,4} = \frac{\omega \mu e^{-jkr}}{4\pi r} 2r_0 I_0$$

$$\cdot (\cos \phi + \sin \phi\, e^{jk \cos \theta\, P/4})$$

1/2-turn helix

$$E_{\phi R1,2} = \frac{-j\omega \mu e^{-jkr}}{4\pi r} 2r_0 I_0$$

$$\cdot \sin \phi\, (e^{jk \cos \theta\, P/2} - 1)$$

$$E_{\phi R3,4} = \frac{\omega \mu e^{-jkr}}{4\pi r} 2r_0 I_0$$

$$\cdot \cos \phi (1 - e^{jk \cos \theta\, P/2})$$

1-turn helix

$$E_{\phi R1,2} = \frac{-j\omega \mu e^{-jkr}}{4\pi r} 2r_0 I_0$$

$$\cdot \sin \phi\, (1 + e^{jkP \cos \theta})$$

$$E_{\phi R3,4} = \frac{\omega \mu e^{-jkr}}{4\pi r} 2r_0 I_0$$

$$\cdot \cos \phi\, (1 + e^{jkP \cos \theta}).$$

Computation

Numerical integration of these expressions with a digital computer provided the theoretical patterns of Fig. 2. The measured patterns plotted for comparison were taken under the conditions outlined in the following section. The experimental patterns are circularly polarized for all θ and ϕ, indicating that E_θ has the same shape as E_ϕ.

EXPERIMENTAL DATA

Radiation Patterns

These details are common in the data of Fig. 3:

measurement frequency	400 MHz
element diameter	0.1 inch
element length	16.0 inches
feed	orthogonal folded baluns; power division and phase quadrature obtained with a directional coupler
mechanical support	0.625-inch diameter aluminum tube provides a balun shield and a shorting point for the distal ends of the elements
geometry	$L_{ax} = N\sqrt{\dfrac{1}{N^2}(16.0'' - 2r_0)^2 - 4\pi^2 r_0^2}.$

Impedance

Limited data indicates a variation in the input impedance at resonance from 70 ohms for the 1/4-turn helix to 15 ohms for the 1-turn helix.

C. C. KILGUS
Appl. Phys. Lab.
The Johns Hopkins University
Silver Spring, Md.

REFERENCES

[1] C. C. Kilgus, "Multielement, fractional turn helices," *IEEE Trans. Antennas and Propagation (Communications)*, vol. AP-16, pp. 499–500, July 1968.
[2] S. A. Schelkunoff, "A general radiation formula," *Proc. IRE*, vol. 27, pp. 660–666, October 1939.

Equatorial Plane Pattern of an Axial-TEM Slot on a Finite Size Ground Plane

The concepts of edge diffraction have been used to compute the scattered and radiated fields of waveguide geometries [1]–[2]. They can also be used to predict the perturbations in the patterns introduced by such features as the edges of a ground plane. Lopez [3] has obtained a rather inaccurate result for the case of a monopole over a circular ground plane. Ryan and Peters [4] have introduced an equivalent current concept to demonstrate that good accuracy can be obtained for this case.

This communication considers a TEM-mode axially slotted ground plane of finite width and length, as shown in Fig. 1. The diffractions from the edges of the ground plane and their contributions to the overall pattern are shown in the computed results. The radiation-pattern calculation will consist of the superposition of rays emanating from the aperture (wedges 1 and 2) and the additional diffracted rays from wedges 3–6 when added in proper relative phase. To check the validity of the technique, experimental results are used for comparison since rigorous solutions do not exist.

The total diffracted field from wedges 1 and 2 including second- and higher order diffractions [1], [2] is given by

$$E_D(r_0,\phi_0) = \frac{e^{-j(kr_0 + \pi/4)}}{\sqrt{2\pi kr_0}} R_D(\phi_0) \quad (1)$$

$$R_D(\phi_0) = e^{j(ka/2) \sin \phi_0}$$

$$\cdot (R_1(\phi_0) + R_2(\phi_0) e^{-jka \sin \phi_0}) \quad (1a)$$

where

$$R_1(\phi_0) = R_{D1}^{(1)}(\phi_0) + R_{D1}^{(h)}(\phi_0) \quad (2)$$

$$R_2(\phi_0) = R_{D2}^{(1)}(\phi_0) + R_{D2}^{(h)}(\phi_0). \quad (2a)$$